Calculating Center-Glass Performance Indices of Windows

John L. Wright, Ph.D., P.Eng.
Member ASHRAE

ABSTRACT

Building envelope performance is strongly influenced by solar gain and heat transfer through windows. The majority of this energy gain or loss passes through the center-glass area of the glazing system. Various methods have been devised to calculate the corresponding center-glass performance indices. Solar heat gain coefficient (SHGC) and U-factor are the quantities most frequently sought. Hand calculations have given way to computer-based techniques. Computer simulation offers the opportunity to employ more detailed models plus the ability to model the large number of glazing systems made possible by design options, such as low-emissivity or solar-control coatings, selective glass tints, substitute fill gases, and glazing layers, that partially transmit longwave radiation. A new, more accurate method is presented in this paper for manipulating spectral optical data while calculating the energy related optical properties of glazing layers and glazing systems. The use of the same technique to track visible and ultraviolet radiation is also demonstrated. In addition, more refined methods are documented for calculating SHGC and U-factor while accounting for the thermal resistance of individual glazings.

INTRODUCTION

Building envelope performance is strongly influenced by solar gain and heat transfer through windows. A one-dimensional simulation can accurately quantify the mechanisms of energy transfer in the center-glass area. The effect of the thermal short circuit caused by edge-seal and frame components must be dealt with using a two- or three-dimensional model. Considerable attention has been devoted to the implementation of edge-glass and frame calculations because of the higher level of complexity involved, but it should be remembered that the center-glass is generally the single component area where the majority of energy gain or loss takes place.

The most important energy-related indices are solar heat gain coefficient (SHGC) and U-factor. Other indices of importance include the solar, visible, and ultraviolet (UV) transmittance values.

Various methods have been devised to calculate center-glass performance indices. Computer simulation offers the ability to conveniently solve the nonlinear problem involving coupled modes of convective and radiative heat transfer. This, in turn, allows for complete examination of the many possible combinations of low-emissivity or solar-control coatings, glass tints, pane spacings, tilts, and substitute fill gases. Computer simulation also provides the capability to properly quantifying the impact of glazing layers that are selective in the solar wavelength band. Many of the newer coatings and tints are strongly selective, and spectral data are now available for almost all commercially available glazing layers.

Two center-glass analysis programs, VISION and WINDOW, are used widely in North America. VISION is specified for energy rating in Canada (CSA 1993), and the WINDOW program is used in the U.S. (NFRC 1991). Early versions of these programs were based on work by Wright (Wright 1980; Hollands and Wright 1980, 1983) and Rubin (1982), respectively. These heat transfer models surpassed previous methods because they introduced the capability of analyzing glazing layers that partially transmit longwave radiation (i.e., diathermanous glazing layers). This is an important feature and its value as a design tool has been demonstrated (Wright 1980, 1985; Wright and Sullivan 1987).

The capabilities of the programs mentioned above have been extended in more recent versions of the software (Wright and Sullivan 1995a; Arasteh et al. 1989; Finlayson et al. 1993). New features include an accounting for the thermal resistance

John L. Wright is associate professor, Department of Mechanical Engineering, University of Waterloo, Ontario, Canada.

of glazing layers and a spectral analysis of the glazing system in the solar wavelengths, allowing for the calculation of visible and UV transmittance plus a more accurate calculation of solar transmittance and SHGC. However, the model extensions incorporated in the two programs are not identical. A wealth of useful information about newer models can be found in consensus standards currently being developed (ASHRAE 1996; ISO 1996), but little detail has been recorded in the technical literature.

This paper provides a record of the most up-to-date models used for center-glass analysis. Information is provided on the way in which these models, or others, are used in the current software, and a discussion regarding the comparison of these models is included. In the particular case of spectral calculations, a new approach is developed offering increased accuracy.

APPROACH

Glazing system energy analysis takes advantage of the fact that there is no appreciable overlap between the band of solar wavelengths below ~3 mm and the band of longer wavelengths by which radiant heat transfer takes place. This naturally leads to a two-step process. First, an optical analysis determines how much of the incident solar radiation is absorbed at each of the glazing layers and how much is transmitted to the indoor space. Second, a heat transfer analysis is used to impose an energy balance on each glazing layer. The net heat transfer from any glazing layer must equal the amount of absorbed solar radiation.

The solar optical calculation can be completed without any information regarding glazing temperatures or heat transfer. The only information from the solar optical step needed in the heat transfer step is the amount of solar radiation absorbed at each glazing layer. These two steps yield the temperature profile and the rate of heat transfer at each glazing layer or interpane gap, which can then be used to determine the center-glass U-factor and SHGC.

Within the two-band framework, it is possible to use a multi-band (i.e., spectral) solar optical model whereby reflected, absorbed, and transmitted amounts of solar radiation are summed by wavelength. Similarly, a spectral calculation can be used to determine other optical properties such as the visible transmittance and ultraviolet transmittance of the glazing system.

SPECTRAL CALCULATIONS

Spectral Data

The glazing system is treated as an n-node array consisting of *n*-2 glazing layers together with the indoor (i=1) and outdoor (*i*=*n*) nodes. This arrangement is shown in Figure 1. It is assumed that each glazing layer is flat and specular.

Three solar optical properties are needed to describe the i^{th} glazing layer, and each should be specified as a function of the wavelength of the incident radiation, λ: (1) the front (outdoor side) reflectance, $\rho_{f,i}(\lambda)$, (2) the back (indoor side) reflectance, $\rho_{b,i}(\lambda)$, and (3) the transmittance, $\tau_i(\lambda)$.

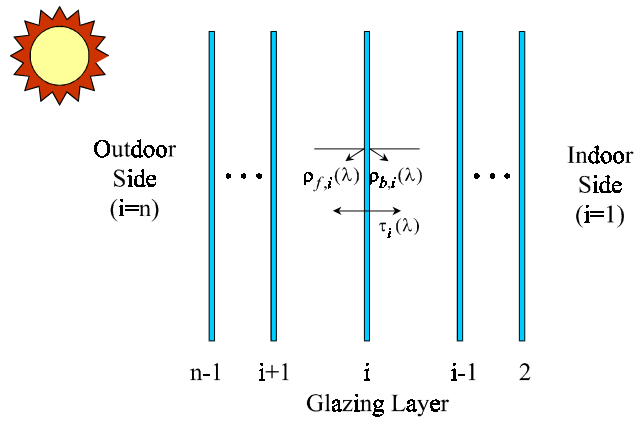

Figure 1 *Numbering arrangement and solar optical properties of glazing layers.*

It is customary to use solar optical properties that pertain to normal incidence, but properties for any given angle of incidence can be used in this analysis to obtain the corresponding set of results. Increased accuracy can be obtained by accounting for the effect of polarization. It is convenient to assume that the incident solar radiation consists of two components (parallel and perpendicular) of equal strength. Measured optical properties pertaining to each of these components are not readily available but can be found on the basis of theory for uncoated glazing layers (e.g., Siegel and Howell 1972) and averaged. More approximate methods can be used for coated glazing layers (Ferguson and Wright 1983; Finlayson et al. 1993). The models presented in this paper could be extended to account individually for the components of polarization, but, in order to concentrate on the spectral calculations, that issue is not pursued.

Note that the spectral optical properties are measured and reported at discrete values of λ (λ_j). All three properties for a given glazing layer are reported at the same values of λ, but the set of λ_j used to describe one glazing layer may not exactly match the sets used for all of the other glazing layers. This is particularly true knowing that spectral data are available from a variety of sources such as measured research data, manufacturers data, and more comprehensive data libraries (e.g., NFRC 1997). Similarly, the solar spectral irradiance, $E(\lambda)$, the photopic response of the eye, $R(\lambda)$, and other functions of interest are tabulated for specific values of λ where, again, each set of λ_j is unique in order to capture the desired level of detail. For example, ASTM Standard E891-87 (air mass 1.5) lists $E(\lambda_j)$ at 121 values of λ_j from 0.305 μm to 4.045 μm, with 34 of those data falling in the visible band for which ASTM Standard E308-90 lists $R(\lambda_j)$ at 81 values of λ_j.

It is assumed that all of the solar spectral curves ($\rho_{f,i}[\lambda]$, $\rho_{b,i}[\lambda]$, $\tau_i[\lambda]$, $E[\lambda]$, etc.) are constructed such that intermediate values can be reliably evaluated by linear interpolation.

alculating Total Optical Properties of a Glazing Layer

Equation 1 shows the way in which any total solar optical property, i.e., P_s, can be determined by averaging the corresponding spectral data, $P(\lambda)$, over the solar wavelength band using $E(\lambda)$ as a weighting function.

$$P_s = \frac{\int_{\lambda=0}^{\infty} P(\lambda)E(\lambda)d\lambda}{\int_{(\lambda=0)}^{\infty} E(\lambda)d\lambda} \quad (1)$$

P_s is called the total (or grey) optical property and is useful because a glazing layer having this property, independent of wavelength, will transmit, reflect, or absorb the same amount of incident solar energy. This can be seen in Equation 1 by recognizing that the integral in the denominator of the right hand side is the total incident flux of radiant energy, I_s.

Equation 1 can be evaluated numerically by replacing the integrals with summations applied over m-1 wavelength bands.

$$P_s = \frac{\sum_{j=1}^{m-1} P(\lambda_{j/j+1})E(\lambda_{j/j+1})\Delta\lambda_j}{\sum_{j=1}^{m-1} E(\lambda_{j/j+1})\Delta\lambda_j} \qquad \Delta\lambda_j = \lambda_{j+1} - \lambda_j \quad (2)$$

where $P(\lambda_{j/j+1})$ and $E(\lambda_{j/j+1})$ are values of P and E, respectively, and are representative of the wavelength band from λ_j to λ_{j+1}.

Several schemes have been formulated for evaluating Equation 2. Each uses the set of λ_j for which $E(\lambda_j)$ data are tabulated. VISION4 subdivides each band from λ_j and λ_{j+1} into four equal subpanels and evaluates representative values of $E(\lambda)$ and $P(\lambda)$ individually by averaging the corresponding values at the endpoints of each subpanel. WINDOW 4.0 evaluates each of $E(\lambda)$ and the $P(\lambda)$ $E(\lambda)$ product at λ_j and λ_{j+1} and uses the average. The ASHRAE draft standard SPC 142 (ASHRAE 1996) specifies that $E(\lambda_{j/j+1})$ and $P(\lambda_{j/j+1})$ be evaluated by calculating each of the corresponding quantities at λ_j and λ_{j+1}, averaging them and then multiplying the two averages to obtain a representative $P(\lambda_{j/j+1})$ $E(\lambda_{j/j+1})$ product.

Each of these schemes entails some approximation. By using the set of λ_j at which the solar irradiance values, $E(\lambda_j)$, are tabulated, $E_i(\lambda_{j/j+1})$ is correctly determined. However, by averaging endpoint values, uncertainty arises in evaluating $P(\lambda_{j/j+1})$ because $P(\lambda)$ may contain discontinuities between λ_j and λ_{j+1}. Figure 2a shows a hypothetical situation that illustrates this point. Furthermore, the $P(\lambda_{j/j+1})$ $E_i(\lambda_{j/j+1})$ product will not be linear between λ_j and λ_{j+1} and may also include discontinuities. Uncertainty in estimating values of $P(\lambda_{j/j+1})$ and the $P(\lambda_{j/j+1})$ $E_i(\lambda_{j/j+1})$ product will be small in most cases, but the size of this error is a function of the particular glazing layers being used and cannot be predicted. It depends on the shapes of the various spectral data curves and the way in which the wavelengths chosen to characterize those curves interact with each other.

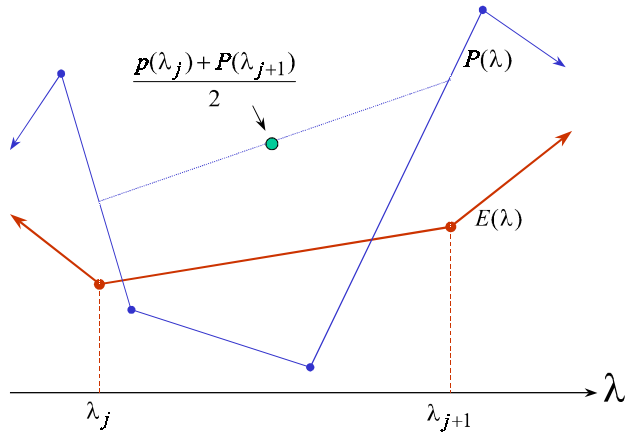

Figure 2a *Discontinuity of optical property,* P(λ)*, within solar radiation band.*

Fortunately, it is possible to formulate a computer algorithm that can be used to evaluate Equation 2 without the uncertainties described above. The critical component of this more accurate approach is the choice of wavelengths used to execute the summation. Instead of using a set of λ_j corresponding to $E(\lambda)$, a larger set of λ_j is assembled that includes all of the wavelengths used in tabulating $E(\lambda)$ and the optical properties of the glazing layer. The larger set of λ_j can readily be assembled using a simple sorting routine. This system of specifying a more detailed set of spectral bands by using the complete set of λ_j will be called the "complete wavelength set" (CWS) method. The CWS wavelengths corresponding to Figure 2a are shown in Figure 2b. The benefit of using the CWS approach is that not only $E(\lambda)$, but all of the optical properties can be taken as linear in order to evaluate each term in the summation. Therefore, within each CWS band:

$$E(\lambda) = a_E + b_E\lambda \quad (3)$$

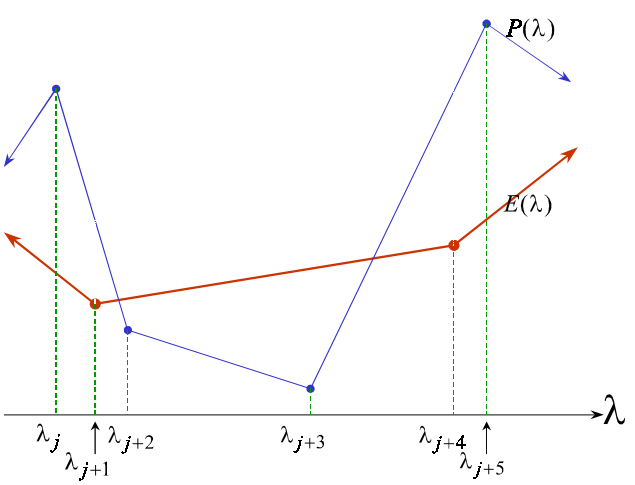

Figure 2b *CWS wavelengths based on* E(λ) *and* P(λ).

and $$P(\lambda) = a_p + b_p\lambda \quad (4)$$

where

$$a_p = P(\lambda_j) - b_p\lambda_j \qquad b_P = \frac{P(\lambda_{j+1}) - P(\lambda_j)}{\lambda_{j+1} - \lambda_j}$$

$$a_E = E(\lambda_j) - b_E\lambda_j \qquad b_E = \frac{E(\lambda_{j+1}) - E(\lambda_j)}{\lambda_{j+1} - \lambda_j}$$

Now the integrals in Equation 1 can be evaluated exactly across each sub-band, and the results from each integration can be summed.

$$P_s = \frac{\sum_{j=1}^{m-1}\left\{\int_{\lambda_j}^{\lambda_j+1}(a_P + b_P\lambda)(a_E + b_E\lambda)d\lambda\right\}}{\sum_{j=1}^{m-1}\left\{\int_{\lambda_j}^{\lambda_j+1}(a_E + b_E\lambda)d\lambda\right\}} \quad (5)$$

Note that *m* now corresponds to the larger set of CWS wavelengths. Evaluating the integrals analytically:

$$P_s = \frac{\sum_{j=1}^{m-1}\{a_P a_E(\lambda_{j+1} - \lambda_j) + \frac{1}{2}(a_P b_E + b_P a_E)(\lambda_{j+1}^2 - \lambda_j^2) + \frac{1}{3}b_P b_E(\lambda_{j+1}^3 - \lambda_j^3)\}}{\sum_{j=1}^{m-1}\{a_E(\lambda_{j+1} - \lambda_j) + \frac{1}{2}b_E(\lambda_{j+1}^2 - \lambda_j^2)\}} \quad (6)$$

Multi-Layer Analysis by the Net Radiation Method

The rate at which radiation of a given wavelength is absorbed in the conditioned space and at each glazing layer can be found by considering the fluxes of radiant energy flowing between the i^{th} and $i{+}1^{th}$ glazings, $I_i^+(\lambda)$ and $I_i^-(\lambda)$. The + and – superscripts denote radiation flowing toward the outdoor and indoor sides, respectively. With reference to Figure 3, it can be seen that the following relations apply.

$$I_i^+(\lambda) = \tau_i(\lambda)I_{i-1}^+(\lambda) + \rho_{f,i}(\lambda)I_i^-(\lambda) \quad i = 1 \text{ to } n-1 \quad (7)$$

$$I_i^-(\lambda) = \tau_{i+1}(\lambda)I_{i+1}^-(\lambda) + \rho_{b,i+1}(\lambda)I_i^+(\lambda) \quad i = 2 \text{ to } n-2 \quad (8)$$

This formulation can be found in a variety of references (e.g., Edwards 1977; van Dijk 1996; Siegel 1973; Shurcliff 1974; Wijeysundera 1975).

With the transmittance of the indoor surfaces set to zero ($\tau_1[\lambda] = 0$), this system of equations can be solved. If the window is considered to be a small surface in a large enclosure, the reflectance of the indoor surfaces can be (and usually is) set to zero ($\rho_{f,1}[\lambda] = 0$). Knowing all values of $I_i^+(\lambda)$ and $I^-(\lambda)$, the portion of incident radiation of wavelength λ, absorbed at the i^{th} glazing layer, $A_i(\lambda)$, is simply

$$A_i(\lambda) = \frac{I_i^-(\lambda) - I_i^+(\lambda) + I_{i-1}^+(\lambda) - I_{i-1}^-(\lambda)}{I_{n-1}^-(\lambda)} \quad (9)$$

The portion transmitted to the indoor space is

$$\tau_{gs}(\lambda) = \frac{I_1^-(\lambda)}{I_{n-1}^-(\lambda)} \quad (10)$$

and the portion reflected from the glazing system is

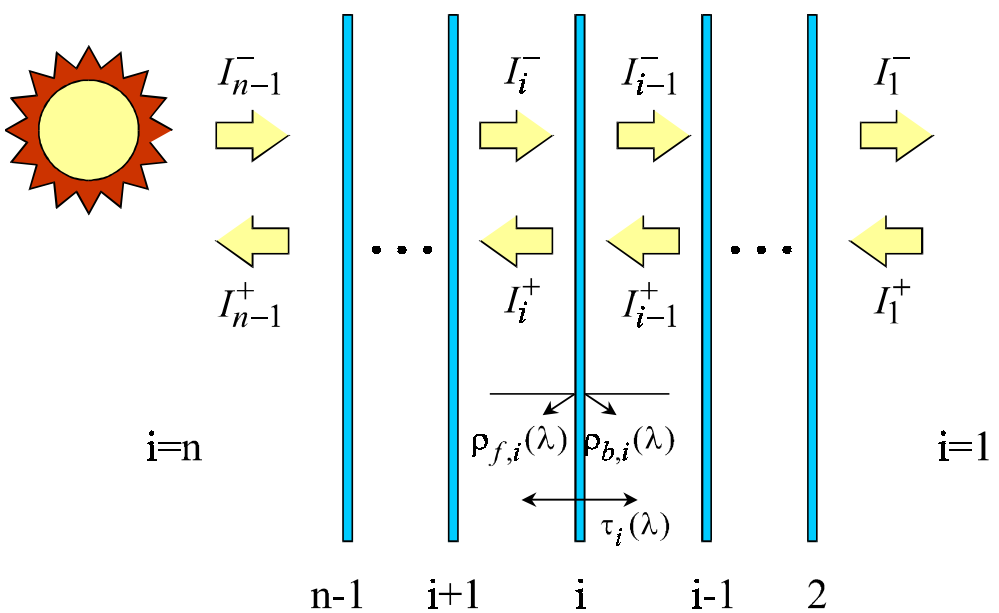

Figure 3 *Solar flux within the glazing system.*

$$\rho_{gs}(\lambda) = \frac{I^{+}_{n-1}(\lambda)}{I^{-}_{n-1}(\lambda)} \tag{11}$$

Note that $I^{-}_{n-1}(\lambda)$, the incident flux, can be set equal to any nonzero value for the purpose of solving Equations 7 through 11.

Solution of the Multi-Layer Model

A variety of methods are available for solving Equations 7 and 8. The most direct approach is matrix reduction, but recursive (e.g., Edwards 1977; Finlayson et al. 1993) solvers can also be used. All solvers must, by necessity, produce the same result. One method is presented in this paper because of its simplicity, ease of implementation, and because it can be easily developed and understood.

"Ray tracing" is used to develop two recursion relations[1] on the basis of the arrangement shown in Figure 4. Consider the effect of adding one more glazing layer, the i^{th} glazing layer, to the outdoor side of an existing glazing system. Assuming that the reflectance of the original glazing system (including multiple internal reflections), r_{i-1}, is known, we seek to determine the reflectance of the glazing system with the i^{th} glazing layer in place (i.e., r_i). Noting that the incident flux on the i^{th} glazing layer is $I^{-}(\lambda)$, the reflected flux can be found by summing the reflected rays. Omitting the spectral notation for convenience, the resulting relation is

$$r_i = \frac{I^{+}_{i}}{I^{-}_{i}} = \rho_{f,i} + \tau_i^2 r_{i-1} + \tau_i^2 r_{i-1}^2 \rho_{b,i} + \tau_i^2 r_{i-1}^3 \rho_{b,i} + \tau_i^2 r_{i-1}^4 \rho_{b,i} + \ldots \tag{12}$$

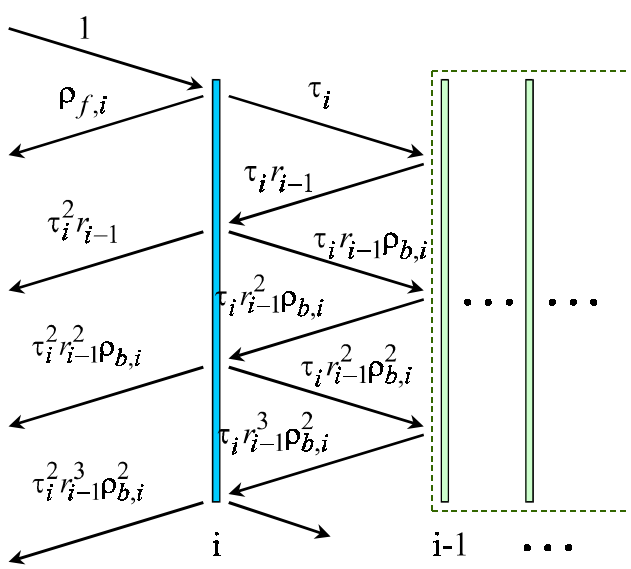

Figure 4 *Ray tracing to develop solar flux analysis.*

1. The development of the same recursion relations using the net radiation method can be found in Edwards (1977).

or $$r_i = \rho_{f,i} + \tau_i^2 r_{i-1} \sum_{j=0}^{\infty} (r_{i-1}\rho_{b,i})^j \tag{13}$$

This can be recognized as a geometric series.

$$\sum_{j=0}^{\infty} x^j = \frac{1}{1-x} \quad \text{for} \quad |x| < 1 \qquad \text{geometric series} \tag{14}$$

so $$r_i = \rho_{f,i} + \frac{\tau_i^2 r_{i-1}}{1 - \rho_{b,i} r_{i-1}} \tag{15}$$

Notice that without any further development, this recursion can be used to calculate all values of r_i by working from $r_1 = \rho_{f,1}$ to r_{n-1}.

Also consider $I^{-}_{i}(\lambda)$ and $I^{-}_{i-1}(\lambda)$, the fluxes of radiation on either side of the i^{th} glazing layer, flowing in the indoor direction. Again, ray tracing can be used to find the ratio between these two quantities, t_i.

(16)

$$t_i = \frac{I^{-}_{i-1}}{I^{-}_{i}} = \tau_i + \tau_i(\rho_{b,i} r_{i-1}) + \tau_i(\rho_{b,i} r_{i-1})^2 + \tau_i(\rho_{b,i} r_{i-1})^3 + \ldots$$

or $$t_i = \frac{\tau_i}{1 - \rho_{b,i} r_{i-1}} \tag{17}$$

Now Equation 17 can be used to obtain t_i from i=2 to i=n-1. The rest of the solution follows by first calculating the flux reflected from the glazing system to the outdoor side $I^{-}_{n-1} = r_{n-1} I^{+}_{n-1}$ and then marching toward the indoor side from i=n-2 to i=1 calculating the remaining fluxes ($I^{-}_{i} = t_{i+1} I^{-}_{i+1}$ and $I^{+}_{i} = r_i I^{-}_{i}$).

CWS Calculation of Solar and Visible Transmittance

The CWS method can be used to calculate the solar transmittance of the glazing system, τ_s. In this case, the CWS wavelength set consists of all the λ_j used to tabulate $E(\lambda)$ and the optical properties of all glazing layers. Assuming that $\tau_{gs}(\lambda)$ is linear over each CWS band, τ_s can be calculated with Equation 6 by setting $P(\lambda)$ equal to $\tau_{gs}(\lambda)$.

The visible transmittance of the glazing system, τ_v, can be calculated using a weighting function that represents the photopic response of the eye, $R(\lambda)$. ASTM Standard E308-90 (ASTM 1990) lists a suitable set of $R(\lambda)$, tabulated as $\bar{y}(\lambda)$, at 81 values of λ from 0.38 μm to 0.78 μm for the CIE 1931 standard observer. The visible transmittance is

$$\tau_v = \frac{\int_{\lambda=0}^{\infty} \tau_{gs}(\lambda) R(\lambda) E(\lambda) d\lambda}{\int_{\lambda=0}^{\infty} R(\lambda) E(\lambda) d\lambda} \tag{18}$$

Using the CWS approach, it is possible to eliminate errors associated with evaluating representative values of $R(\lambda)$ (i.e., errors caused by any mismatch between the wavelengths at which $R(\lambda)$, $E(\lambda)$, and the optical properties of glazing layers are reported). Replacing $R(\lambda)$ with

$$R(\lambda) = a_R + b_R\lambda \tag{19}$$

and assuming $$\tau_{gs}(\lambda) = a_\tau + b_\tau\lambda \tag{20}$$

Equation 18 becomes

$$\tau_v = \frac{\sum_{j=1}^{m-1}\left\{\begin{array}{l} a_E a_\tau a_R(\lambda_{j+1}-\lambda_j) + \\ \frac{1}{2}(a_E a_\tau b_R + a_E b_\tau a_R + b_E a_\tau a_R)\left(\lambda_{j+1}^2-\lambda_j^2\right) + \\ \frac{1}{3}(a_E b_\tau b_R + b_E a_\tau b_R + b_E b_\tau a_R)\left(\lambda_{j+1}^3-\lambda_j^3\right) + \frac{1}{4}b_E b_\tau b_R\left(\lambda_{j+1}^4-\lambda_j^4\right) \end{array}\right\}}{\sum_{j=1}^{m-1}\left\{\begin{array}{l} a_R a_E(\lambda_{j+1}-\lambda_j) + \\ \frac{1}{2}(a_R b_E + b_R a_E)\left(\lambda_{j+1}^2-\lambda_j^2\right) + \\ \frac{1}{3}b_R b_E\left(\lambda_{j+1}^3-\lambda_j^3\right) \end{array}\right\}} \tag{21}$$

In this case, m corresponds to a set of λ_j consisting of all the λ_j used to tabulate $R(\lambda)$, $E(\lambda)$, and the optical properties of all glazing layers. Note that the magnitude of m can be reduced substantially by accepting only the wavelengths where $R(\lambda)$ is nonzero (i.e., 0.38 μm ≤ λ ≤ 0.78 μm) and by stripping out duplicate values of λ_j.

CWS Calculation of Ultraviolet Transmittance

The UV transmittance of the glazing system, τ_{uv}, can be calculated according to Equation 18 simply by replacing $R(\lambda)$ with a weighting function, $\Gamma(\lambda)$, that restricts the calculation to the UV wavelengths. For example, the UV band used in WINDOW 4.0 (Finlayson et at. 1993) is specified by

$$\begin{array}{ll} \Gamma(\lambda) = 1 & 0.3\mu m \le \lambda \le 0.39\mu m \\ \Gamma(\lambda) = 0 & \text{otherwise} \end{array} \tag{22}$$

Thus, the calculation of τ_{uv} can be carried out using Equation 21 with $R(\lambda)$ replaced by $\Gamma(\lambda)$. This is equivalent to applying Equation 6 (with $P[\lambda] = \tau_{gs}[\lambda]$) to the range of λ, where $\Gamma(\lambda)$ is nonzero. The set of m wavelengths used to evaluate τ_{uv} will be relatively small because values of λ_j falling outside the range where $\Gamma(\lambda)$ is nonzero can be excluded.

It is common to choose $\Gamma(\lambda)$ such that greater weight is given to the more damaging radiation at shorter wavelengths. The Krochman "UV relative damage factor" can be used for this calculation (Krochman 1978).

$$\begin{array}{ll} \Gamma(\lambda) = e^{12.28-25.56\lambda} = 2153.46e^{-25.56\lambda} & 0.3\mu m \le \lambda \le 0.5\mu m \\ \Gamma(\lambda) = 0 & \text{otherwise} \end{array} \tag{23}$$

If $\Gamma(\lambda)$ is of the form $\Gamma(\lambda) = \alpha e^{-\beta\lambda}$ and $\tau_{sg}(\lambda)$ is assumed to be linear in each CWS band, the damage weighted UV transmittance can be calculated as

$$\tau_{duv} = \frac{\sum_{j=1}^{m-1}\left\{\begin{array}{l} \frac{a_\tau a_E}{\beta}\left(e^{-\beta\lambda_{j+1}}-e^{-\beta\lambda_j}\right) + \\ \frac{a_\tau b_E + a_E b_\tau}{(\beta)^2}\left(e^{-\beta\lambda_{j+1}}(\beta\lambda_{j+1}+1)-e^{-\beta\lambda_j}(\beta\lambda_j+1)\right) \end{array}\right\}}{\sum_{j=1}^{m-1}\left\{\begin{array}{l} \frac{a_\tau a_E}{\beta}\left(e^{-\beta\lambda_{j+1}}-e^{-\beta\lambda_j}\right) + \\ \frac{b_E}{(\beta)^2}\left(e^{-\beta\lambda_{j+1}}(\beta\lambda_{j+1}+1)-e^{-\beta\lambda_j}(\beta\lambda_j+1)\right) \end{array}\right\}} \tag{24}$$

Note that α does not appear in the final expression because it can be cancelled from numerator and denominator. Only β remains, which, for the Krochman damage function, is $\beta = 25.56\ \mu m^{-1}$.

CWS Calculation of Absorbed Solar Flux

The absorbed solar flux at the i^{th} glazing layer appears in the heat transfer analysis and is denoted S_i. The amount of solar radiation of wavelength λ within an infinitesimal wavelength band, $d\lambda$, and absorbed at the i^{th} glazing layer, dS_i, is

$$dS_i = A_i(\lambda)E(\lambda)d\lambda \tag{25}$$

Summing over all wavelengths,

$$S_i = \int_{\lambda=0}^{\infty} A_i(\lambda)E(\lambda)d\lambda \tag{26}$$

Equation 26 must be evaluated numerically.

$$S_i = \sum_{j=1}^{m-1} A_i(\lambda_{j/j+1})E(\lambda_{j/j+1})\Delta\lambda_j \qquad \Delta\lambda_j = \lambda_{j+1}-\lambda_j \tag{27}$$

where $A_i(\lambda_{j/j+1})$ and $E_i(\lambda_{j/j+1})$ are values of A_i and E_i, respectively, that are representative of the wavelength band from λ_j to λ_{j+1}.

Several schemes have been formulated for evaluating Equation 27, and each uses the set of λ_j for which $E(\lambda_j)$ data are tabulated. Each of these schemes entails some amount of error for the same reasons previously discussed.

Using CWS yields a result similar to the numerator of Equation 6. Specifically, assuming $A_i(\lambda)$ is linear in each CWS band,

$$A_i(\lambda) = a_A + b_A\lambda \tag{28}$$

then

$$S_i = \sum_{j=1}^{m-1}\left\{a_A a_E(\lambda_{j+1}-\lambda_j) + \frac{1}{2}(a_A b_E + b_A a_E)(\lambda_{j+1}^2-\lambda_j^2) + \frac{1}{3}b_A b_E(\lambda_{j+1}^3-\lambda_j^3)\right\} \tag{29}$$

The portion of the total incident solar flux, I_s, absorbed at the i^{th} glazing layer is simply $A_i = S_i/I_s$.

Comments Regarding the CWS Method

The CWS approach of undertaking spectral integrations is an important step forward. It may be argued that existing methods leave little room for improvement, but the magnitude of the error resulting from discontinuities in spectral data curves cannot be known in general. This error will be greater in some cases than in others. The CWS approach eliminates the error caused by discontinuities.

The calculation of total optical properties for individual glazing layers is free of error when CWS integration is used. The calculation of glazing system transmittance and SHGC values retains a very small amount of error because $\tau_{gs}(\lambda)$ and $A_i(\lambda)$ are assumed to be linear over each CWS panel. This is a particularly safe assumption because of the finer resolution of the CWS panels and because discontinuities no longer present any difficulty. Integration of strongly nonlinear functions could easily be handled by subdivision of the CWS panels. Note that the one strongly nonlinear function used in center-glass analysis, the Krochman UV relative damage factor, can be incorporated analytically (i.e., without error) in the CWS analysis.

HEAT TRANSFER CALCULATION

Overview

Center-glass heat flux can be quantified using a straightforward analysis of coupled conductive, convective, and radiative heat transfer. It is assumed that each glazing layer possesses grey longwave (i.e., λ>3 µm) optical properties. Radiative heat exchange between glazing layers and conductive heat transfer within each glazing layer can be described using fundamental relations. Calculations of convective heat transfer require the use of correlations based on experimental data.

The governing equations are sufficiently general to permit each glazing layer to have asymmetric radiative properties and to account for the absorption of solar energy in each of the individual glazing layers. However, the most significant difference between this and previous hand-calculation methods is that any or all of the glazing layers can be diathermanous. This feature is unimportant for glazing layers made of glass, but a plastic film may partially transmit longwave radiation if it is sufficiently thin. This phenomenon can adversely affect the thermal performance of a glazing system but can also be used to its advantage (Wright 1985; Wright and Sullivan 1987).

The analysis presented here also accounts for the thermal resistance of the glazings themselves.

Governing Equations

Figure 5 shows the i^{th} glazing in an array of glazing layers. Three longwave optical properties are needed to describe each glazing layer: the front and back surface emissivities, $\varepsilon_{f,i}$ and $\varepsilon_{b,i}$, and the transmittance, t_i. The values of four variables are

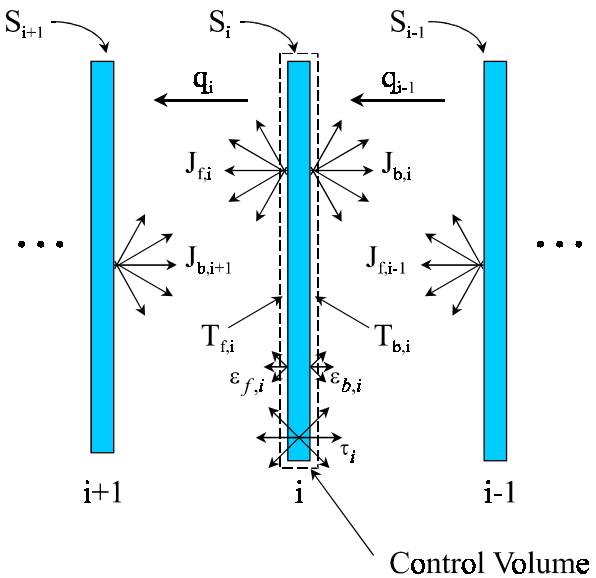

Figure 5 *Glazing layer arrangement for heat transfer analysis.*

sought at each glazing layer. These are the temperatures of the outdoor and indoor facing surfaces, $T_{f,i}$ and $T_{b,i}$, plus the radiant fluxes leaving the outdoor and indoor facing surfaces (i.e., the radiosities), $J_{f,i}$ and $J_{b,i}$. If these quantities are known, the heat flux across the i^{th} gap, q_i, can be calculated by summing the convective and radiative components of heat transfer. The convective component is quantified in terms of the convective heat transfer coefficient, h_i, and the radiative flux is simply the difference between the radiosities of the two surfaces facing the gap. Thus,

$$q_i = h_i[T_{f,i} - T_{b,i+1}] + J_{f,i} - J_{b,i+1} \tag{30}$$

The solution can be generated by applying the following four equations at each glazing:

$$h_i[T_{f,i} - T_{b,i+1}] + J_{f,i} - J_{b,i+1} = S_i + h_{i-1}[T_{f,i-1} - T_{b,i}] + J_{f,i-1} - J_{b,i} \tag{31}$$

$$J_{f,i} = \varepsilon_{f,i}\sigma T_{f,i}^4 + \tau_i J_{f,i-1} + \rho_{f,i} J_{b,i+1} \tag{32}$$

$$J_{b,i} = \varepsilon_{b,i}\sigma T_{b,i}^4 + \tau_i J_{b,i+1} + \rho_{b,i} J_{f,i-1} \tag{33}$$

$$T_{b,i} - T_{f,i} = \frac{t_{gl,i}}{2k_{gl,i}}(2q_{i-1} + S_i) \tag{34}$$

where $t_{gl,i}$ is the thickness and $k_{gl,i}$ the conductivity of the i^{th} glazing layer.

Equation 31 describes an energy balance imposed at the surfaces of the i^{th} glazing layer. Recall that S_i is the flux of solar radiation absorbed at the i^{th} glazing layer.

Equations 32 and 33 define the radiant fluxes leaving the surfaces of the i^{th} glazing layer in terms of the glazing layer surface temperatures and other radiosities. Each radiosity consists of three components: emitted, transmitted, and reflected radiant flux. The reflectance values used in these equations ($\rho_{f,i} = 1 - \tau_i - \varepsilon_{f,i}$ and $\rho_{b,i} = 1 - \tau_i - \varepsilon_{b,i}$) should not

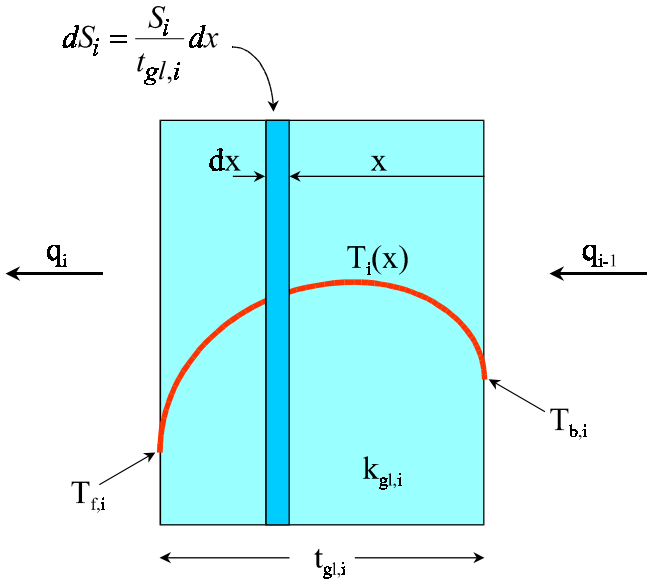

Figure 6 *Energy balance within glazing layer.*

be confused with similar variables used in the solar optical analysis.

The temperature difference across the i^{th} glazing is given by Equation 34. This expression results from an energy balance accounting for absorbed solar energy and conduction within the glazing. Consider a layer of thickness, *dx*, at a distance, *x*, from the back (indoor facing) surface of the glazing layer (Figure 6). If it is assumed that the solar energy is absorbed uniformly through the thickness of the glazing, an energy balance can be applied to this control volume.

$$-k_{gl,i}\frac{\partial T}{\partial x}\bigg|_x + \frac{S_i}{t_{gl,i}}dx = -k_{gl,i}\frac{\partial T}{\partial x}\bigg|_{x+dx} \tag{35}$$

or

$$\frac{\partial^2 T}{\partial x^2} = \frac{-S_i}{k_{gl,i}t_{gl,i}} \tag{36}$$

Integrating twice and applying the boundary conditions

$$-k_{gl,i}\frac{\partial T}{\partial x}\bigg|_{x=0} = q_{i-1} \quad \text{and} \quad -k_{gl,i}\frac{\partial T}{\partial x}\bigg|_{x=t_{gl}} = q_i$$

yields Equation 34.

An interesting by-product of the derivation is an expression for the temperature profile through the glazing:

$$T_i(x) = \left[\frac{S_i}{2k_{gl,i}t_{gl,i}}\right]x^2 + \left[\frac{T_{f,i}-T_{b,i}}{t_{gl,i}} + \frac{S_i}{2k_{gl,i}}\right]x + T_{b,i} \tag{37}$$

It should be noted that this analysis is based on the assumption that the glazing layer is opaque to longwave radiation. It is possible to develop a more detailed model that is applicable to diathermanous glazing layers by considering both solar and longwave radiation absorbed within the glazing layer. However, the only diathermanous layers are thin plastic films where neither the temperature drop nor the temperature profile through the film are of importance. This more detailed model can also be used to distinguish between solar radiation absorbed through the body of the glazing layer and at the glazing layer surfaces (i.e., where a coating has been applied), but optical data regarding the split between these two contributions are not available.

It is possible to neglect the thermal resistance of the glazings by setting the right-hand side of Equation 34 to zero as if $k_{gl,i} = \infty$. In this case, the glazing is a uniform temperature, and Equations 34 and 35 reduce to $T_{f,i} = T_{b,i} = T_i(x)$. Earlier formulations were of this type (i.e., based on Equations 31, 32, and 33 only) and are described in Wright (1980), Hollands and Wright (1980, 1983), and Rubin (1982). The more detailed model described in the previous paragraph has been incorporated in VISION3 (Wright and Sullivan 1992) and VISION4 (Wright and Sullivan 1995a). An example is shown in Figure 7, where the temperature profile through the outdoor glazing is curved because it is tinted but the profile through the indoor glazing is very nearly linear because it is clear glass and absorbs relatively little solar radiation. More recent versions of WINDOW account for the thermal resistance of glazing layers by including a temperature node at the center plane of each glazing layer where it is assumed that all of the solar radiation is absorbed (Arasteh et al. 1989; Finlayson et al. 1993).

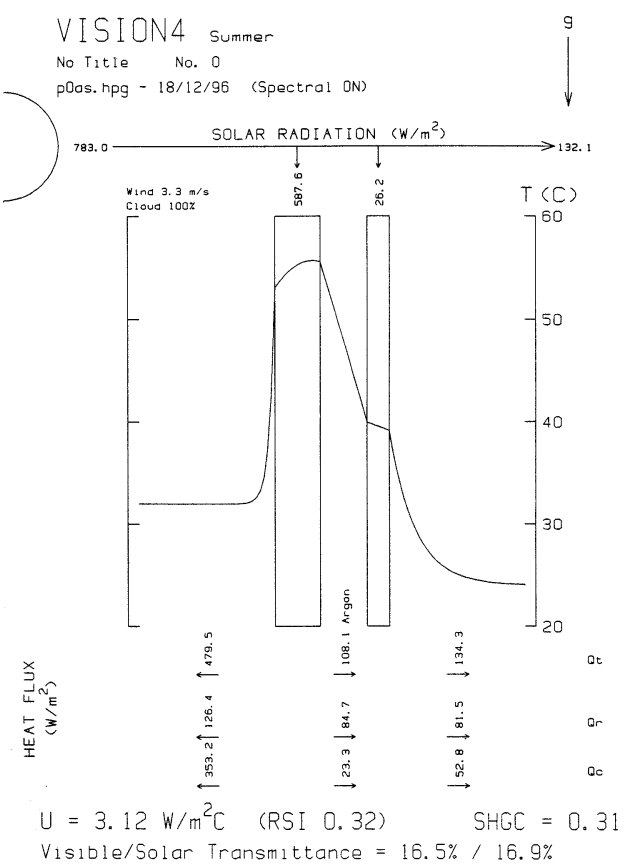

Figure 7 *Example of temperature profile through glazing layer.*

This approach does not lead to a continuous expression for the temperature profile through the glazing layer.

The remaining pieces needed to complete the heat transfer model can be found in the literature. The best source is the ASHRAE Standard 142P (ASHRAE 1996). Information can be found regarding the effect of radiant exchange with the outdoor environment under partly cloudy conditions, correlations needed to quantify indoor, outdoor, and glazing cavity convective heat transfer coefficients, and the properties of fill gases and fill gas mixtures.

Solution of the Heat Transfer Model

In all, 4*n*-6 independent simultaneous equations can be written on the system, comprised of *n*-2 energy balances on glazing layers, *n*-2 energy balances within glazing layers, and 2*n*-2 radiosity equations. The equations contain terms in temperature ($T_{f,i}$ and $T_{b,i}$) and black emissive power ($E_{b,f,i} = \sigma T^4_{f,i}$ and $E_{b,b,i} = \sigma T^4_{b,i}$) and, hence, are nonlinear even before account is taken of the fact that each h_i depends on the relevant temperature level and temperature difference.

If the temperature difference across each glazing layer, $T_{b,i}$–$T_{f,i}$, and the convective heat transfer coefficients, h_i, are held constant, the governing equations become linear but only if solved in terms of black emissive power instead of temperature. Thus, two new quantities are defined. The convective heat transfer coefficient based on emissive power, $\hat{h}_i$, is

$$\hat{h}_i(E_{b,f,i} - E_{b,b,i+1}) = h_i(T_{f,i} - T_{b,i+1}) \quad (38)$$

and the drop in black emissive power through a glazing layer, $\Delta E_{b,i}$, is

$$\Delta E_{b,i} = E_{b,b,i} - E_{b,f,i} \quad (39)$$

Now Equations 31 to 34 can be cast in matrix form, $AX = B$. The elements of matrix A and column vector B are those given in Table 1, and X is a column vector whose transpose is

$$X_t = (J_{f,1}, J_{b,2}, E_{b,b,2}, E_{b,f,2}, J_{f,2}, \ldots J_{b,i}, E_{b,b,i}, E_{b,f,i}, J_{f,i}, \ldots J_{b,n-1}, E_{b,b,n-1}, E_{b,f,n-1}, J_{f,n-1}, J_{b,n}) \quad (40)$$

The solution algorithm is comprised of the following steps.

1. An initial guess for glazing layer temperatures (i.e., $T_{b,i} = T_{f,i} = (T_{b,n} + T_{f,1})/2$) is made.
2. All $\Delta E_{b,i}$ are set to zero.
3. The corresponding sets of h_i and $\hat{h}_i$ are calculated.
4. The A matrix and B vector terms are calculated.
5. The solution vector X is found by some suitable solver yielding sets of black emissive powers from which new sets of $T_{f,i}$'s and $T_{b,i}$'s can be found.
6. The new sets of $T_{f,i}$'s and $T_{b,i}$'s are compared to the old sets. If each member is not equal to the corresponding member of the old set, to within some acceptable bound (e.g., 10^{-4} K), the new sets are used to replace the old sets and the solution procedes to the third step.

When returning to the third step, it is necessary to update each value of $\Delta E_{b,i}$. VISION4 completes this step using:

$$\Delta E_{b,i} = \sigma\left\{\left(\frac{T_{b,i} + T_{f,i}}{2} + \frac{T_{b,i} - T_{f,i}}{2}\right)^4 - \left(\frac{T_{b,i} + T_{f,i}}{2} - \frac{T_{b,i} - T_{f,i}}{2}\right)^4\right\} \quad (41)$$

where the mean glazing layer temperature, $(T_{b,i} + T_{f,i})/2$, is calculated using the current glazing layer temperatures and the temperature drop through the glazing layer, $T_{b,i} - T_{f,i}$, is calculated using Equation 34. The temperatures shown in Equation 41 can be cancelled to give

$$\Delta E_{b,i} = \sigma(T^4_{b,i} - T^4_{f,i}) \quad (42)$$

TABLE 1
Elements of Matrix A and Vector B

		Column	4*i*-8	4*i*-7	4*i*-6	4*i*-5	4*i*-4	4*i*-3	4*i*-2	4*i*-1	
i	**Row**	**Restriction**	**A Matrix**								**B Vector**
1	1							1			$E_{b,f,1}$
	4*i*-6			$-\rho_{b,i}$	1	$-\varepsilon_{b,i}$			$-\tau_i$		0
2	4*i*-5					1	−1				$\Delta E_{b,i}$
		n=3		1	−1	$-\hat{h}_1$	$-\hat{h}_2$	−1	1	$-\hat{h}_2$	$-S_2 - \hat{h}_1 E_{b,f,1} - \hat{h}_2 E_{b,b,3}$
to	4*i*-4	*i*=2		1	−1	$-\hat{h}_1$	$-\hat{h}_2$	−1	1		$-S_2 - \hat{h}_1 E_{b,f,1}$
		i=*n*–1	$\hat{h}_{i-1}$	1	−1	$-\hat{h}_1$	$-\hat{h}_1$	−1	1		$-S_i - \hat{h}_i E_{b,b,n}$
n–1		other	$\hat{h}_{i-1}$	1	−1	$-\hat{h}_1$	$-\hat{h}_1$	−1	1	$-\hat{h}_1$	$-S_i$
	4*i*-3			$-\tau_i$			$-\varepsilon_{f,i}$	1	$-\rho_{f,i}$		0
n	4*n*-6				1						$\varepsilon_{b,n} E_{b,b,n}$

All entries for the A matrix and B vector can be generated from this table by letting *i* run from 1 to *n*. Entries not listed in this table should be set to zero. Entries falling outside the range of the A matrix may be disregarded.

showing that the approximate nature of Equation 41 disappears as convergence is reached.

ENERGY RELATED INDICES OF MERIT

Center-Glass U-Factor

The center-glass U-factor, U_c, can be determined for any environmental condition involving indoor/outdoor temperature difference and any level of incident solar radiation. It can be expressed as the reciprocal of the total center-glass thermal resistance, R_{tot},

$$U_c = \frac{1}{R_{tot}} \tag{43}$$

where R_{tot} is found by summing the individual thermal resistance values of the glazing cavities and glazing layers from the indoor side to the outdoor side.

$$R_{tot} = \sum_{i=1}^{n-1} R_{gap,i} + \sum_{i=2}^{n-1} R_{gl,i} \tag{44}$$

The thermal resistance of the i^{th} glazing cavity is

$$R_{gap,i} = \frac{T_{f,i} - T_{b,i+1}}{q_i} \tag{45}$$

and the thermal resistance of the i^{th} glazing layer is

$$R_{gl,i} = \frac{t_{gl,i}}{k_{gl,i}} \tag{46}$$

The exception to Equation 45 is the resistance on the outdoor side of the glazing system, $R_{gap,n-1}$, where, for conditions other than fully cloudy conditions, the extra cooling caused by radiant exchange with the clear portions of the sky must be considered. In this case, the effective ambient temperature, T_{ae}, must be used instead of the outdoor air temperature, $T_{b,n}$ (ASHRAE 1996; Wright and Sullivan 1992, 1995a).

Center-Glass Solar Heat Gain Coefficient

The center-glass solar heat gain coefficient, SHGC, can be found by summing the directly transmitted solar gain and the absorbed/redirected solar gain (Wright and Sullivan 1995b).

$$\text{SHGC} = \tau_s + \frac{1}{I_s} \sum_{i=2}^{n-1} N_i S_i \tag{47}$$

where I_s is the incident solar flux and N_i is the portion of S_i that is redirected by heat transfer to the indoor space (i.e., the inward flowing fraction).

Equation 47 suggests that SHGC cannot be calculated for a condition with no solar radiation ($I_s = 0$), but this is not true. Recognizing that $S_i = A_i I_s$, Equation 47 becomes

$$\text{SHGC} = \tau_s + \sum_{i=2}^{n-1} N_i A_i \tag{48}$$

Also, recognizing that $N_1 = 1$ and $A_1 = \tau_s$, Equation 48 can be written as

$$\text{SHGC} = \sum_{i=1}^{n-1} N_i A_i \tag{49}$$

The inward flowing fraction, N_i, is known to be equal to the ratio of the thermal resistance from the location of the absorbed solar radiation to the outdoor side and the total indoor/outdoor thermal resistance. For example, if most of the thermal resistance comprising R_{tot} exists between the i^{th} glazing and the outdoor side, then most of S_i will make its way to the indoor space.

If the thermal resistance of the glazing layers is neglected, N_i can be calculated by considering only the glazing cavity resistances:

$$N_i = \frac{\sum_{j=i}^{n-1} R_{gap,j}}{R_{tot}} \tag{50}$$

However, if the thermal resistance of the glazing layers is included, the calculation of N_i is more involved. Consider an infinitesimal layer within the i^{th} glazing layer of thickness, dx, and at distance, x, from the indoor side of the glazing layer. This arrangement is shown in Figure 8. If the thermal resistance between the outdoor environment and the outdoor side of the glazing layer is R_{out} and the flux of solar radiation absorbed within dx is dS_i, the inward flowing flux, dq_{in}, will be

$$dq_{in} = \frac{R_{out} + \frac{t_{gl,i} - x}{k_{gl,i}}}{R_{tot}} dS_i \tag{51}$$

Substituting

$$dS_i = \frac{S_i}{t_{gl,i}} dx \tag{52}$$

and summing through the thickness of the glazing layer,

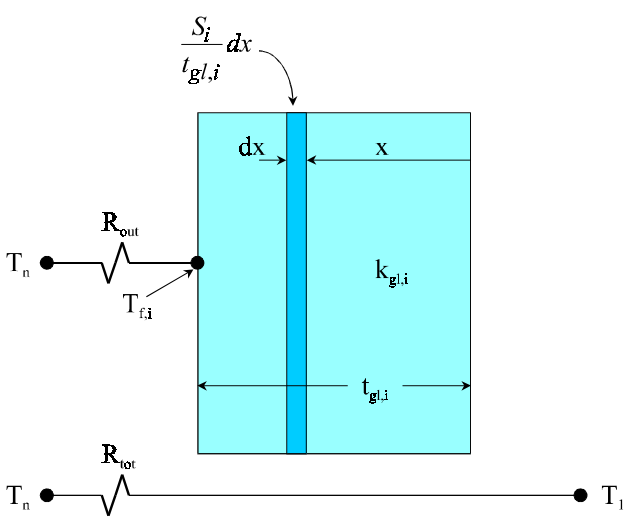

Figure 8 *Calculating the inward flowing fraction of absorbed solar radiation from a glazing layer with thermal resistance.*

$$q_{in} = \frac{S_i}{R_{tot} t_{gl,i}} \int_{x=0}^{t_{gl,i}} R_{out} + \frac{t_{gl,i} - x}{k_{gl,i}} dx \tag{53}$$

Solving

$$\frac{q_{in}}{S_i} = N_i = \frac{R_{out} + \frac{1}{2}\frac{t_{gl,i}}{k_{gl,i}}}{R_{tot}} \tag{54}$$

Thus, given the assumption that solar radiation is absorbed uniformly through the glazing layer, N_i can be calculated as if the solar radiation were absorbed at the midplane of the glazing layer. Therefore, no discrepancy between VISION4 (based on uniform distribution) and WINDOW 4.0 (based on solar absorption at the midplane) exists because of the way in which N_i is calculated.

Finally, the full expression for N_i can be written as

$$N_i = \frac{\sum_{j=i}^{n-1} R_{gap,j} + \sum_{j=i+1}^{n-1} \frac{t_{gl,j}}{k_{gl,j}} + \frac{1}{2}\frac{t_{gl,i}}{k_{gl,i}}}{R_{tot}} \tag{55}$$

CONCLUSIONS

An up-to-date model has been presented for calculating the center-glass performance indices of windows. This procedure includes several important components.

1. A new solar spectral calculation, the complete wavelength set (CWS) method, has been formulated. The CWS approach is free of almost all of the uncertainty inherent in previous methods and is completely free of uncertainty caused by discontinuities and wavelength mismatches in data describing optical properties and spectral weighting functions.

2. A comprehensive heat transfer model has been specified in full detail. Step-by-step instructions have been provided for using linear matrix reduction methods to solve the nonlinear governing equations.

3. Details regarding the calculation of all indices of merit, optical and energy related, are presented and discussed. Singularities in calculating the U-factor when adjacent glazing layers are at the same temperature, or in calculating SHGC when no solar radiation exists, have been avoided.

4. All energy related calculations account for the thermal resistance of individual glazings. It has also been shown that the assumption of uniform vs. center-plane absorption of solar radiation within a glazing layer has no bearing on the calculation of solar gain.

Sufficient information has been provided so that the solution method is readily programmable by the potential user.

ACKNOWLEDGMENTS

This research was supported by NRCan (Natural Resources Canada) and the Department of Mechanical Engineering, University of Waterloo.

REFERENCES

Arasteh, D., S. Reilly, and M. Rubin. 1989. A versatile procedure for calculating heat transfer through windows. *ASHRAE Transactions* 95(2): 755-765.

ASHRAE. 1996. BSR/ASHRAE Standard 142P (Public Review Draft), Standard method for determining and expressing the heat transfer and total optical properties of fenestration products. Atlanta: American Society of Heating, Refrigerating and Air-Conditioning Engineers, Inc.

ASTM. 1990. *ASTM Standard, Designation: E308-90, Standard test method for computing the colors of objects by using the CIE system*. Philadelphia: American Society for Testing and Materials.

CSA. 1993. *CSA A440.2-93, Energy performance evaluation of windows and sliding glass doors*. Rexdale, Ontario, Canada: Canadian Standards Association.

Edwards, D.K. 1977. Solar absorption by each element in an absorber-coverglass array. *Solar Energy*, 19: 401-402.

Ferguson, J., J.L. Wright. 1983. *VISION: A computer program to evaluate the thermal performance of super windows*. Solar Energy Program, National Research Council Canada, Report No. Passive 10.

Finlayson, E.U., D.K. Arasteh, C. Huizenga, M.D. Rubin, and M.S. Reilly. 1993. *WINDOW 4.0: Documentation of calculation procedures*. Energy and Environment Division, Berkeley, Calif.: Lawrence Berkeley Laboratory.

Hollands, K.G.T., and J.L. Wright. 1980. Theory and experiment on heat loss coefficients for plastic covers, pp. 441-445. Proceedings of the American Section of the International Solar Energy Society, Phoenix.

Hollands, K.G.T. and J.L. Wright. 1983. Heat loss coefficients and effective $\alpha\tau$ products for flat plate collectors with diathermanous covers. *Solar Energy*, 30 (3): 211-216.

ISO. 1996. ISO Standard 15099 (Working Draft No. 1), TC 163/WG2, Windows and doors—Thermal transmission properties—Detailed calculations. Geneva: International Organization for Standardization.

Krochman, J. 1978. Zur frage der beleuchtung von museen. *Lichttechnik* 1(2): 66-70, *Lichttechnik* 2(3): 104-105.

NFRC. 1991. *NFRC 100-91, Procedure for determining fenestration product thermal properties (currently limited to U-values)*. Silver Spring, Md.: National Fenestration Rating Council.

NFRC. 1997. *NFRC spectral data library #4 for use with the Window 4.1 computer program*, LBL-35298, TA-315, Addendum #4.

Rubin, M. 1982. Calculating heat transfer through windows. *Energy Research*, 6: 341-349.

Siegel, R. 1973. Net radiation method for transmission through partially transparent plates. *Solar Energy*, 15: 273-276.

Siegel, R., and J.R. Howell. 1972. *Thermal radiation heat transfer.* New York: McGraw Hill.

Shurcliff, W.A. 1974. Transmittance and reflection loss of multi-plate window of a solar radiation collector: Formulas and tabulations of results for the case of n=1.5. *Solar Energy*, 16: 149-154.

van Dijk, H.A.L., J. Goulding. (eds.) 1996. WIS reference manual (updated draft), TNO Building and Construction Research.

Wijeysundera, N.E. 1975. A net radiation method for the transmittance and absorptivity of a series of parallel regions. *Solar Energy*, 17: 75-77.

Wright, J.L. 1980. Free convection in inclined air layers constrained by a v-corrugated Teflon film. M.A.Sc. thesis, University of Waterloo, Mechanical Engineering Department, Waterloo, Canada.

Wright, J.L. 1985. The computer simulation of super window glazing systems which incorporate Teflon (FEP) inner glazings. *Proc. ISES/SESCI Intersol '85*, Montreal, Canada, Vol. 1, pp. 267-271.

Wright, J.L., and H.F. Sullivan. 1987. Simulation and measurement of windows with low emissivity coatings used in conjunction with Teflon inner glazings. *ISES Solar World Congress*, Hamburg, West Germany, September, Vol. 4, pp. 3136-3140.

Wright, J.L., and H.F. Sullivan. 1992. *VISION3 glazing system thermal analysis—Reference manual*. Advanced Glazing System Laboratory, Department of Mechanical Engineering, University of Waterloo, Waterloo, Ontario, Canada.

Wright, J.L., and H.F. Sullivan. 1995a. *VISION4 glazing system thermal analysis—Reference manual.* Advanced Glazing System Laboratory, Department of Mechanical Engineering, University of Waterloo, Waterloo, Ontario, Canada.

Wright, J.L. 1995b. Summary and comparison of methods to calculate solar heat gain. *ASHRAE Transactions* 101(1): 802-818.